Ultra-Compact (80 mm^2) Differential-Mode Ultra-Wideband (UWB) Bandpass Filters with Common-Mode Noise Suppression

Paris Vélez, *Member IEEE*, Jordi Naqui, *Member IEEE*, Armando Fernández-Prieto, Jordi Bonache, *Member IEEE*, Javier Mata-Contreras, Jesús Martel, *Member IEEE*, Francisco Medina, *Fellow IEEE*, and Ferran Martín, *Fellow IEEE*

Abstract— **This paper presents a novel approach for the implementation of balanced ultra-wideband (UWB) bandpass filters with common-mode noise suppression. To a first-order approximation, the differential-mode filter response is described by the canonical circuit model of a bandpass filter, i.e., a cascade of series-connected resonators alternating with shunt-connected parallel resonant tanks. Thus, the series branches of the balanced filter are implemented by means of inductive strips and patch capacitors, whereas the shunt sections are realized through mirrored stepped impedance resonators (SIRs) and low-impedance (i.e., capacitive) short transmission line sections. For the differential-mode, the symmetry plane is a virtual ground, the wide strip sections of the SIRs are effectively grounded, and the SIRs behave as grounded inductors parallel connected to capacitors. However, for the common-mode, where the symmetry plane is an open (magnetic wall), the SIRs act as shunt-connected series resonators, thus providing transmission zeros at their resonance frequencies. By properly tailoring the location of these transmission zeros, rejection of the common-mode over the differential filter pass band can be achieved. To illustrate the potential of the approach, an order-5 balanced bandpass filter covering the regulated band for UWB communications (3.1 GHz-10.6 GHz) is designed and fabricated. The filter exhibits common-mode rejection above 10 dB over the whole differential filter passband, with differential-mode insertion losses lower than 1.9 dB and return losses better than 10 dB. Since the proposed design approach is based on planar semi-lumped components, filter size is as small as 10.5 mm×7.6 mm.**

Index Terms– **Differential filters, ultra-wideband (UWB), common-mode suppression, stepped impedance resonator (SIR), microstrip technology.**

I. INTRODUCTION

THE design of differential-mode bandpass filters with common-mode noise suppression is of high interest in balanced circuits, where high immunity to environmental noise, interference and crosstalk between different elements are key advantages over their single-ended counterparts. Several strategies for the implementation of balanced bandpass filters with common-mode rejection have been proposed [1]-[13]. Essentially, such filters are designed by using symmetry properties. Namely, their topologies are symmetric structures where the electric wall of the symmetry plane for the differential-mode makes the structure to exhibit band pass functionality. However, through a proper design, it is possible to achieve common-mode rejection in the differential filter pass band thanks to the effects of the magnetic wall for the common-mode.

Based on these ideas, dual-band [2]-[5], moderate or narrow band [6],[7], wideband [9],[10], and ultra-wideband (UWB) [11]-[13] balanced filters have been recently reported. Most of these common-mode suppressed balanced filters are based on distributed elements, and filter optimization requires parametric analysis. This is the case, for instance, of the UWB balanced filters implemented by means of branch line sections with open-circuited stubs attached along the symmetry plane [11] or by means of open-ended parallel coupled lines [12]. Other UWB balanced filters based on signal interference techniques are reported in [14],[15].

In [16], the authors presented a novel approach for the design of balanced wideband bandpass filters with common-mode noise suppression. The balanced filters reported in [16] are described by the circuit model depicted in Fig. 1(a). For the differential-mode, the symmetry plane is a virtual ground, resulting in the circuit of Fig. 1(b). Conversely, the symmetry plane is an open-circuit for the common-mode, and the equivalent circuit for that mode is the one depicted in Fig. 1(c). In the circuits of Fig. 1, the shunt resonators are coupled through admittance inverters. In practice, such inverters have been implemented by means of meandered differential lines (with differential-mode characteristic admittance $J_{i,i+1}$, with $i = 1,2...$), whereas the elements of the shunt branches have been implemented by combining mirrored stepped impedance resonators (SIRs) and low-impedance transmission line

sections. The SIRs are described by the inductances L_{pi} and the capacitances C_{zi}; the capacitances C_{pi} are implemented through electrically short low-impedance transmission line sections. Through this approach, order-3 and order-5 balanced quasi-Chebyshev bandpass filters with excellent common-mode noise suppression were demonstrated [16]. In those filters, the agreement between circuit simulation, electromagnetic simulation and measurement is remarkable. This aspect is very interesting for design purposes. However, the approach presented in [16] has two drawbacks, mainly related to the presence of the distributed admittance inverters: (i) filter size, and (ii) the limited fractional bandwidth. In this paper, the main aim is to replace the admittance inverters of the filters reported in [16] with semi-lumped resonators, with an eye towards achieving ultra-wideband (UWB) differential-mode responses and optimizing filter dimensions. The accurate circuit model of the new proposed filters, including parasitics, is presented and used for design purposes. Finally, a fifth order balanced filter roughly covering the regulated band for UWB communications (3.1 GHz - 10.6 GHz) is designed and fabricated.
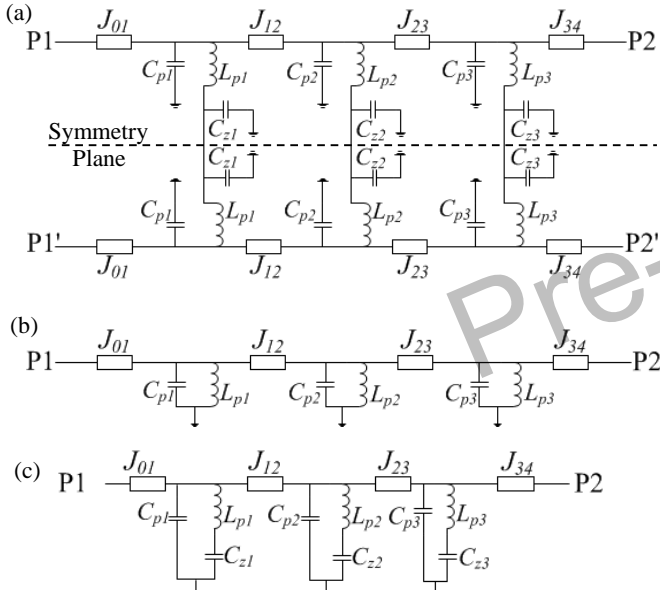

Fig. 1. Circuit model of the balanced bandpass filters with common-mode suppression proposed in [16] (a), and equivalent circuits for the differential (b) and common (c) modes.

The paper is organized as follows: section II is focused on the topology and circuit model (including validation) of the proposed balanced UWB filters. The design methodology is presented in section III, whereas the reported prototype and characterization results are presented in section IV. In section V, the performance and dimensions of the proposed filter are compared to those of other reported balanced UWB bandpass filters. Finally, the main conclusions are highlighted in section VI.

II. FILTER TOPOLOGY, CIRCUIT MODEL AND VALIDATION

The topology of the shunt branches of the proposed differential-mode UWB bandpass filter is similar to the one reported in [16] (Fig. 2): a pair of mirrored SIRs, and two

electrically short low-impedance transmission line sections acting as grounded capacitors. For moderate or wide band bandpass filters, this topology is accurately described by the elements of the shunt branches in the circuit of Fig. 1(a). However, for an accurate description of the structure over extremely wide bands (i.e., from 3.1 GHz up to 10.6 GHz), it is necessary to add series connected inductances to the model of the shunt branch, as shown in Fig. 2(b). These inductances (denoted by L_{par}) must be considered parasitic elements, but their presence is mandatory for an accurate description of the shunt branch through a lumped element equivalent circuit model over the regulated UWB band. To demonstrate the validity of the proposed model, we have extracted the parameters of the circuit of Fig. 2(b) for the topology depicted in Fig. 2(a). To this end, we have inferred the S-parameters of the structure for the differential- and common-modes through full wave electromagnetic simulation, using the *Agilent Momentum* commercial software (see Fig. 3). The considered substrate is *Rogers RO3010* with dielectric constant ε_r=10.2 and thickness h=254 μm. From the differential-mode S-parameters, we have obtained the reactance of the series and shunt branch of the equivalent T-circuit model according to standard formulas [17]. The results are depicted in Fig. 4. Determination of C_p and L_p has been done from the resulting resonance frequency of the shunt reactance of the T-model (where the shunt reactance exhibits a singularity) and from the reactance slope at that frequency. L_{par} has been directly inferred from the slope of the series reactance. Finally, the capacitance C_z has been inferred from the position of the transmission zero frequency for the common-mode, given by:

$$f_Z^{cc} = \frac{1}{2\pi} \frac{1}{\sqrt{C_z L_p}} \tag{1}$$

Notice that in Figs. 3 and 4, the agreement between the results inferred from electromagnetic and circuit simulation (the element values are indicated in the caption of Fig. 3) are reasonably good up to frequencies beyond the range of interest (3.1 GHz – 10.6 GHz). Therefore, these results validate the proposed model and point out the need to include the parasitic inductance L_{par} (not considered in [16]) for an reasonable description of the structure. The circuit simulation without parasitic inductance (L_{par}) is also included in Fig. 3(a) for comparison purposes.
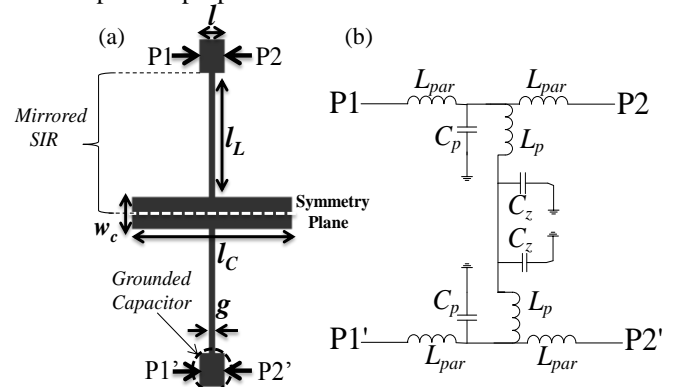

Fig. 2. Typical topology (a) and lumped element equivalent circuit model (b) of the shunt branches of the proposed balanced UWB bandpass filter. Dimensions are: l= 0.56 mm, g= 0.14 mm, l_L=2.65 mm, l_C= 3.6 mm and w_C= 0.68 mm.
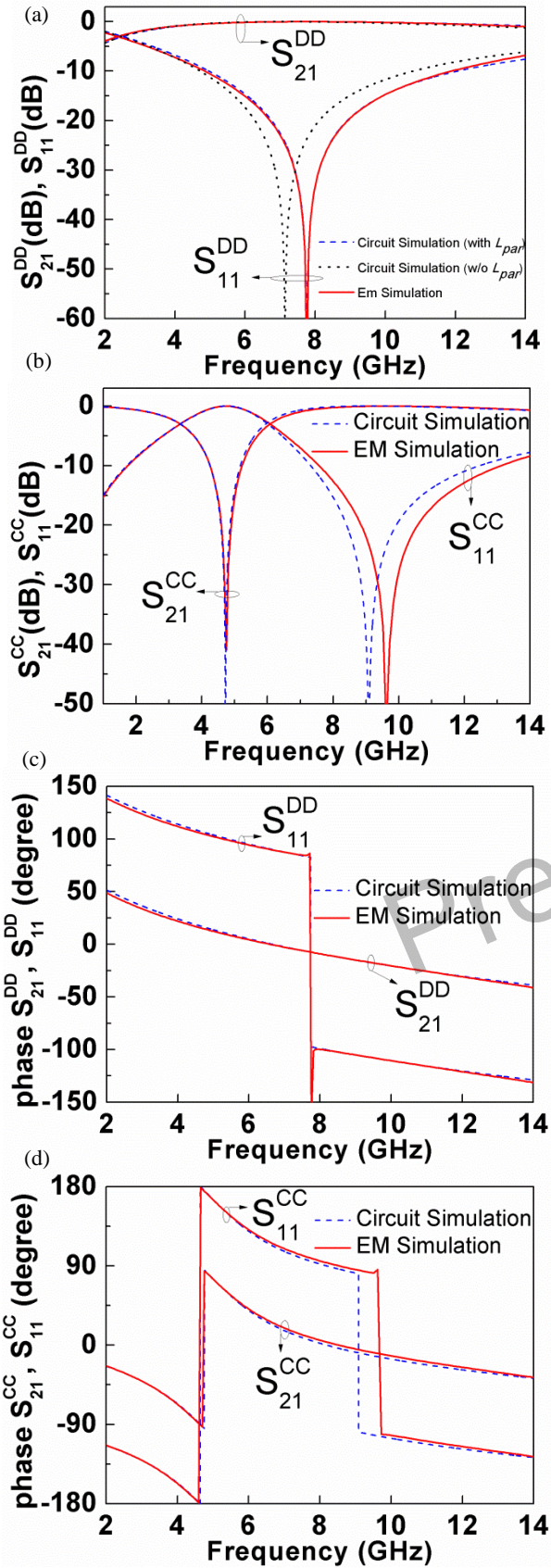
Fig. 3. *S*-parameters for the structure of Fig. 2 inferred from electromagnetic and circuit simulation. (a) Magnitude for differential-mode, (b) magnitude for common-mode, (c) phase for differential-mode, (d) phase for common-mode. The element values of the circuit model of Fig. 2(b) are: L_{par}=0.069 nH, C_p= 0.35 pF, L_p=1.42 nH, C_z=0.8 pF.
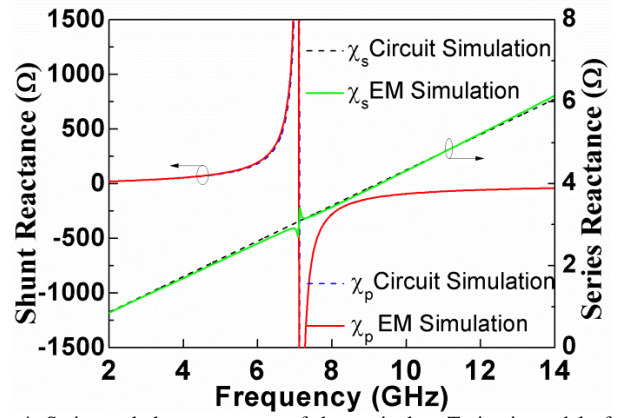

Fig. 4. Series and shunt reactance of the equivalent T-circuit model of the structure of Fig. 2(a) for the differential-mode inferred from electromagnetic and circuit simulation. The element values are those indicated in the caption of Fig. 3.

The key differential aspect between the UWB bandpass filters presented here and the wideban filters reported in [16] concerns the series branches. In order to achieve UWB filter responses, and simultaneously small size, the admittance inverters are replaced with series resonators. Thus, with exception of element parasitics (L_{par} plus the parasitics of the series branches, to be discussed later), the proposed filters are roughly described by the canonical circuit model of a bandpass filter (i.e., a cascade of series resonators alternating with shunt resonant tanks) [18]. As it is well known from filter theory, both the capacitance of the series branches and the inductance of the shunt branches increase with filter bandwidth. Conversely, the inductance of the series branches and the capacitance of the shunt branches are small for bandpass filters with very wide bandwidths. This means that, in order to achieve the required bandwidth (3.1 GHz – 10.6 GHz), the capacitance of the series branch must be necessarily large.

The typical required values have forced us to implement such capacitors by means of patch capacitances (we first unsuccessfully considered the use of interdigital capacitors). Therefore, ground plane etching has been necessary to accommodate such capacitors. Metallic vias can in principle be avoided by series-connecting two identical patch capacitances. However, this strategy increases the required capacitor area since each individual capacitance value is twice the nominal one. We have thus opted for implementing the series capacitances through an optimized topology (in terms of size) that uses a metallic connection between the upper and lower metal levels (via). The series inductance of the series branches (of small value for UWB filters) is simply implemented by means of a pair of short inductive strips cascaded to the capacitor terminals. Nevertheless, the presence of the vias may contribute to the series inductance as well. The top and 3D views of a typical series resonator are depicted in Figs. 5(a) and (b), respectively.

Unfortunately, the lumped element equivalent circuit model of the series branch is not so simple [see Fig. 5(c)]. Notice that since the pairs of series resonators replacing the admittance inverters in the circuit of Fig. 1(a) are very distant, the differential- and common-mode circuits describing such structures are undistinguishable and given by the circuit

model describing the isolated resonators [Fig. 5(c)]. Notice also that the proposed resonator is asymmetric with regard to the ports [see Fig. 5(a) and (b)]. Such asymmetry is accounted for by the proposed circuit model by considering different parasitic inductances (L_{LCs1} and L_{LCs2}) and capacitances (C_{par1} and C_{par2}).
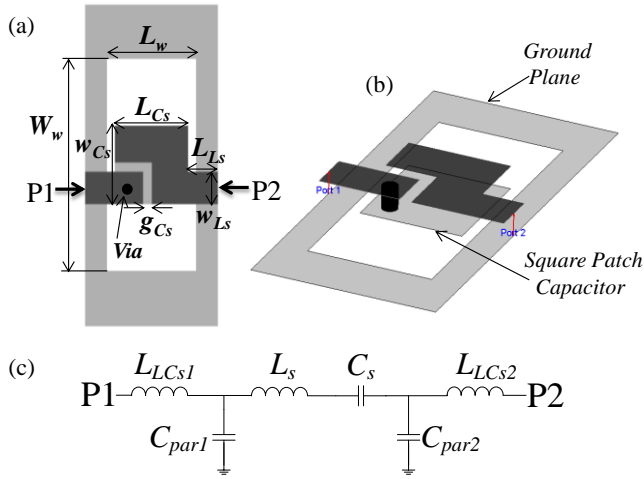

Fig. 5. Top view (a), 3D view (b), and lumped element equivalent circuit model (c) of the series branches of the proposed balanced UWB bandpass filter. Dimensions are: W_w=3.3 mm, L_w=1.46 mm, w_{Ls}=0.5 mm, L_{Ls}=0.49 mm, w_{Cs}=1.22 mm, L_{Cs}=1.2 mm and g_{Cs}=0.144 mm.

By using the *Agilent Momentum* full wave simulator, we have obtained the *S*-parameters of the structure depicted in Fig. 5 (see Fig. 6), and from these parameters, the series reactance and the shunt reactances of the equivalent π-circuit model have been inferred. Such reactances are depicted in Fig. 7, where they are compared with the reactances derived from the transformation of the model of Fig. 5(c) to its equivalent π-circuit model. It is remarkable that the shunt reactances of the equivalent π-circuit model are unequal, confirming the need to consider an asymmetric circuit model (i.e., such reactances are significantly different) to describe the series resonator. Notice also that in certain frequency regions the right-hand side shunt reactance exhibits negative slope. This does not contradict the Foster reactance theorem [19], since the curves depicted in Fig. 7, rather than corresponding to reactances of circuits with identifiable reactive elements, they are the reactances of an equivalent circuit (π-circuit model), and such a circuit may not be described by lumped elements (this is indeed our case).

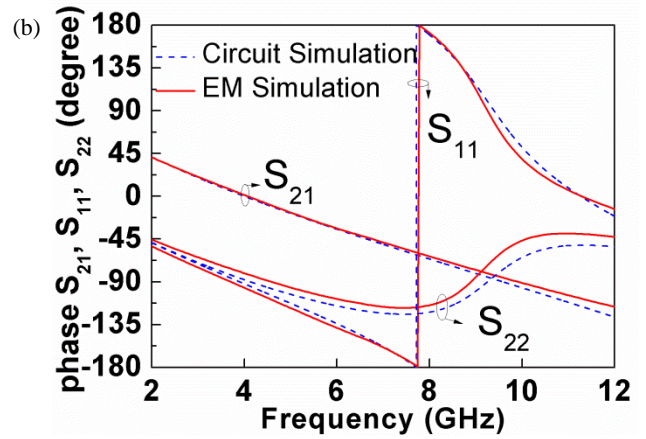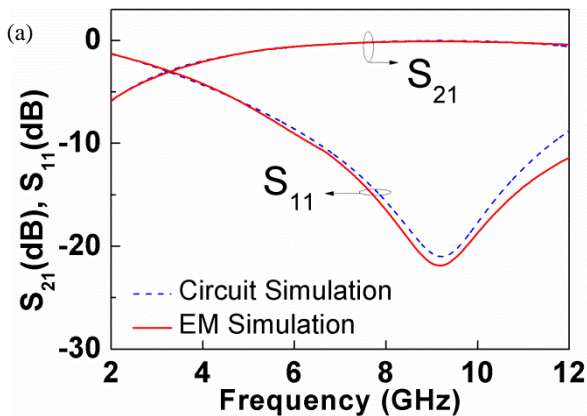

Fig. 6. *S*-parameters (magnitude (a) and phase (b)) for the structure of Fig. 5 inferred from electromagnetic and circuit simulation. The element vales of the circuit model of Fig. 5(c) are: C_s=0.453 pF, L_s=1.39 nH, C_{par1}=0.33 pF, L_{LCs1}=0.31 nH, C_{par2}=0.18 pF, L_{LCs2}=0.123 nH. The magnitude of S_{22} is roughly undistinguishable from that of S_{11} and is not depicted.
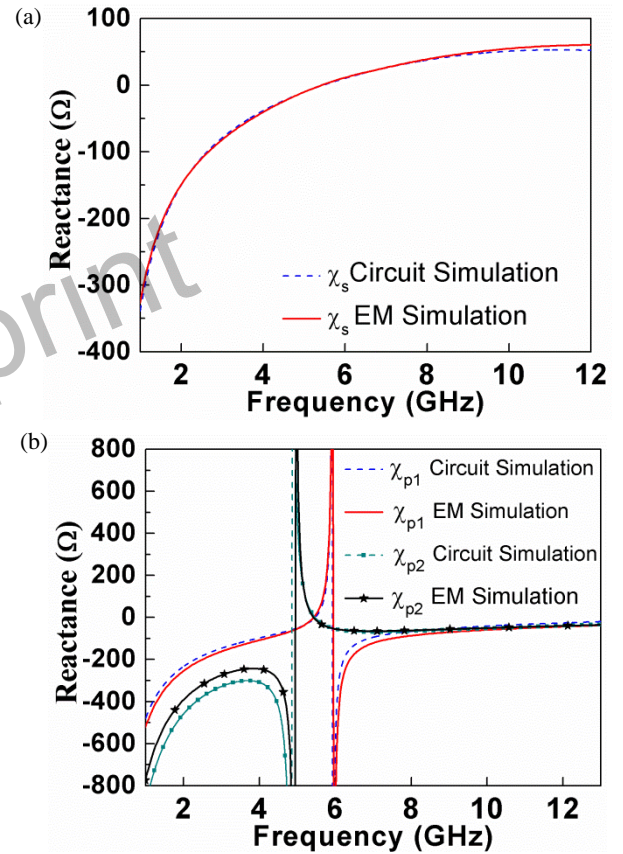
Fig. 7. Series (a) and shunt (b) reactances of the equivalent π-circuit model of the structure of Fig. 5(a) inferred from electromagnetic and circuit simulation. The element values are those indicated in the caption of Fig. 6.

The agreement between the results inferred from electromagnetic and circuit simulation in Figs. 6 and 7 is very reasonable and validates the proposed circuit model. The determination of the circuit parameters is not so straightforward, as compared to the shunt branch. For the series branch, the procedure to obtain the circuit parameters is as follows: first of all, in the low frequency limit, the inductances can be neglected, and the resulting model is a capacitive asymmetric π-circuit model. Thus by representing the susceptances of the series and shunt branches, the

capacitors C_{par1}, C_{par2} and C_s can be inferred from the susceptance slope in the DC limit. Once these element values are known, the inductances are determined by curve fitting the reactances of the three branches of the equivalent circuit model.

III. DESIGN OF THE PROPOSED UWB BALANCED BANDPASS FILTERS

Filter design is oriented towards achieving a Chebyshev response for the differential-mode with the strongest possible rejection of the common-mode over the differential filter pass band. The key idea to reject the common-mode is to locate the transmission zeros, related to the SIRs, at different positions over the differential filter pass band (notice that the series branches do not have any influence on the position of these transmission zeros). Since the inductances of the narrow strips of the SIRs are determined from the specifications of the differential-mode filter response, it follows that the transmission zero locations must be controlled through the dimensions of the wide capacitive sections of the SIRs. According to the model of the shunt branch [Fig. 2(b)], each branch provides one transmission zero for the common-mode. Typically, three transmission zeros are enough in order to achieve a significant common-mode rejection over the regulated UWB band (this is the case of the proposed filter, as will be later shown). Filter design is a two-step process where first the layout that provides the required differential mode response is obtained. This excludes the determination of the patch capacitors (described by the capacitances C_z). Then, the dimensions of these patch capacitances are determined in order to set the transmission zeros for the common-mode and thus achieve a stop band for that mode over the differential filter pass band.

Let us now focus on the design of the balanced filter in order to cover the regulated UWB band for the differential-mode. The intended filter response for the differential-mode is an order-5 Chebyshev response covering the band from 3.1 GHz up to 10.6 GHz with a ripple of 0.15 dB. By considering the canonical order-5 bandpass filter circuit model with shunt connected parallel resonators at the first, third, and fifth stages, and series connected series resonators at the second and fourth stages, the element values giving such a response are: $C_1 = C_5 = 0.535$ pF, $L_1 = L_5 = 1.44$ nH, $C_2 = C_4 = 0.532$ pF, $L_2 = L_4 = 1.448$ nH, $C_3 = 0.888$ pF, $L_3 = 0.868$ nH where the sub-index denotes the filter stage. Once these values are known, the next step is to independently synthesize the layouts for each filter stage (shunt and series branches) with an eye towards achieving the above element values for the active elements of the filter model for the differential-mode (active elements are those reactive elements in the models of Figs. 2(b) and 5(c) not being the parasitic elements, namely, C_{pi}, L_{pi}, C_{si}, and L_{si}). The parameter extraction procedure explained before is used for that purpose, and optimization at the layout level is done as specified next.

For the shunt branches, the dimensions of the patch capacitors (C_{pi}) and inductive strips (L_{pi}) are estimated from the formulas providing the dimensions of the low- and high-impedance transmission line sections of stepped-impedance low pass filters. Then, optimization is carried out at layout level in order to obtain the required element values for C_{pi} and L_{pi} from the parameter extraction procedure detailed before. Notice that parameter extraction gives also the value of the parasitic inductance L_{par}.

For the series branches, we consider a square geometry for the patch capacitor, a via with a diameter of 0.1mm, and 0.5mm wide access lines. Then the area of the square capacitor and the length of the access lines are tuned until the active elements C_s and L_s, inferred from parameter extraction and curve fitting as specified before, are those corresponding to the ideal Chebyshev response. This procedure provides also the parasitic elements of the series branch.

Obviously, due to the presence of the parasitic elements, we do not expect that the filter response for the differential mode agrees with the ideal Chebyshev response. Thus, the filter layout must be modified in order to obtain a better approximation to the required Chebyshev response. The key aspect in our design process is to assume that layout tuning does not substantially modify the parasitic elements. Therefore, the next step is to set the parasitic elements in the circuit model to those values inferred from parameter extraction and curve fitting, and tune the active elements until the filter response for the differential-mode agrees with the intended Chebyshev response to a good approximation in the band of interest. Notice that this is a tuning at the circuit level. Nevertheless, since there are too many degrees of freedom, tuning may be complex and time consuming, unless an automatic process is considered. We have thus implemented an automatic optimization routine in *Agilent ADS* in order to find the element values that provide a minimum in-band return loss level (10 dB) with the frequency positions of the 5 matching points (reflection zeros) as close as possible to those of the ideal Chebyshev response. This routine gives the active element values of the filter circuit model. Once these elements are known, the next step is to modify (tune) the layout in order to infer these element values from parameter extraction and curve fitting for either filter stage. It is worth mentioning that synthesis is not excessively complex since the number of geometrical free parameters per filter stage is small. The element values, including parasitics, are given in table I (notice that the first and fifth stage are slightly different).

As it was already mentioned, the wide patch capacitances of SIRs determine the position of the transmission zeros for the common-mode, but they do not have any influence on the differential filter response. Thus, with exception of such capacitances, filter layout is determined from the design method detailed above. For which concerns the patches corresponding to the grounded capacitances, C_z, we have determined their area in order to obtain transmission zeros for the common-mode at the following frequencies: 5.5 GHz, 7 GHz and 10 GHz.

IV. PROTOTYPE DEVICE AND RESULTS

The layout and photograph of the designed filter are depicted in Fig. 8. The filter has been fabricated by means of a standard photo/mask etching technique in the *Rogers RO3010* substrate with dielectric constant $\varepsilon_r = 10.2$ and thickness $h = 254$ μm. The differential and common-mode

filter responses are depicted in Fig. 9. Due to the presence of parasitics, the measured and electromagnetically simulated differential filter responses are a rough approximation of the ideal Chebyshev response (also included in the figure). Indeed filter selectivity at the upper edge is degraded as compared to that of the ideal Chebyshev response as consequence of the optimization criterion indicated above (in-band return loss closest as possible to those of the ideal Chebyshev). However the selectivity at the lower band edge is good, and this aspect is important since many applications require strong rejection of interfering signals at low frequencies (i.e., below 3.1 GHz). There is a good agreement between the lossless electromagnetic simulation, and the circuit simulation (including parasitics) of the differential filter response [see Fig. 9(a)]. This further validates the proposed circuit model and the design procedure explained before. The electromagnetic simulation with losses and the measurement [Fig. 9(b)] are also in reasonable agreement. The measured insertion loss for the differential-mode is better than 1.9 dB between 3.1 GHz and 10.6 GHz, whereas the return loss is higher than 10 dB within the same frequency interval. The slight discrepancies in the insertion loss are mainly attributed to the effects of the connectors and soldering (a more accurate TRL differential calibration, complex in this case, could be necessary). The common-mode response is reasonably predicted by the circuit model (common-mode), as depicted in Fig. 9(c). Thanks to the presence of three transmission zeros, a common-mode rejection better than 10dB over the whole regulated UWB has been achieved. Concerning dimensions, these are as small as 10.5 mm × 7.6 mm, that is $0.5\lambda \times 0.37\lambda$ (excluding the tapered access lines), λ being the guided wavelength at the central filter frequency. The differential group delay, shown in Fig. 10, exhibits a value smaller than 0.5 ns in the whole differential pass band, and a variation smaller than 0.28 ns.

TABLE I
CIRCUIT ELEMENTS FOR THE EQUIVALENT CIRCUIT OF THE DIFFERENTIAL UWB FILTER (PARASITIC ELEMENTS ARE INDICATED IN GREY). THE UNITS ARE nH FOR THE INDUCTANCES AND pF FOR THE CAPACITANCES.

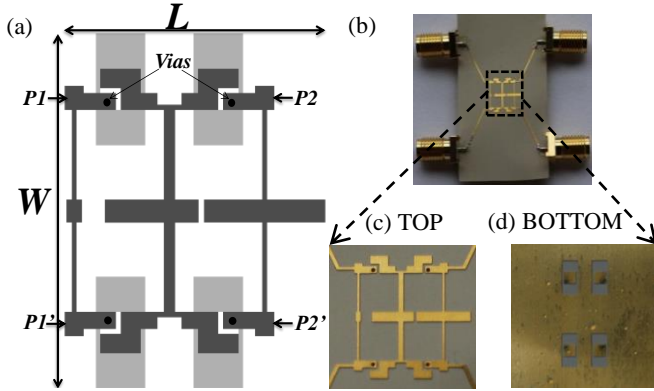| i	L_p	C_p	L_{par}	L_s	C_s	L_{LCs1}/L_{LCs2}	C_{par1}/C_{par2}
1	1.44	0.38	0.06				
2,4				1.25	0.48	0.31/0.09	0.30/0.23
3	0.87	0.47	0.16				
5	1.46	0.40	0.11				

(a)

(b)

(c)

Fig. 8. Layout (a) and photograph (b) of the fabricated filter. A zoom of the photograph is shown in (c) top view and (d) bottom view. Dimensions are: W = 10.5 mm and L = 7.6 mm.
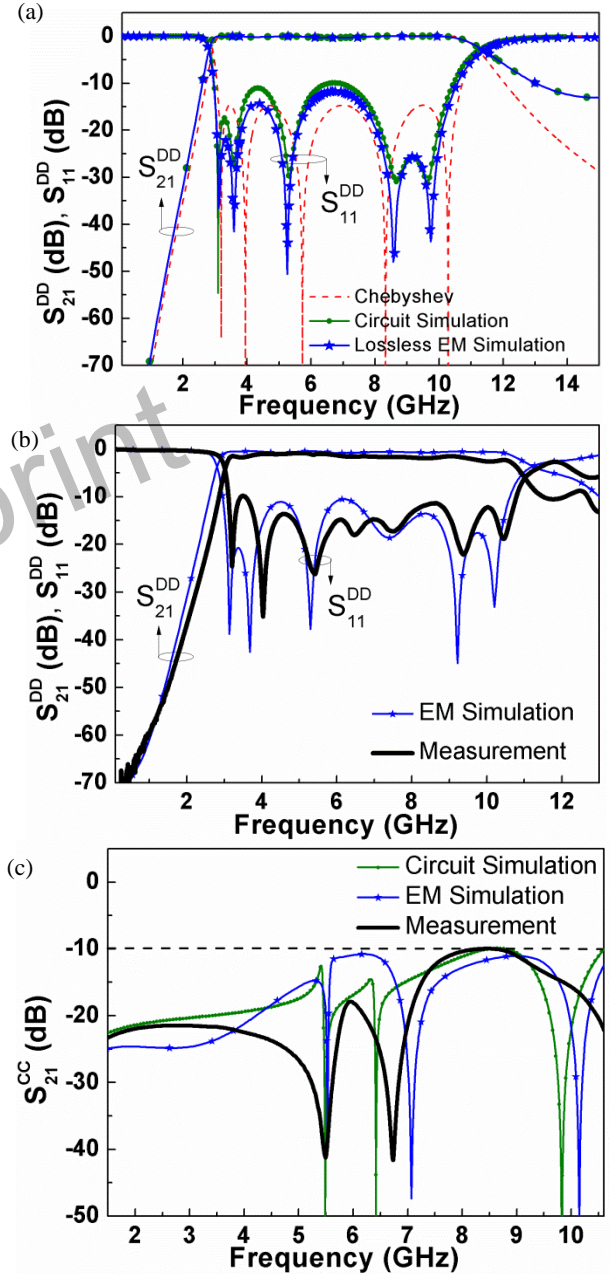
Fig. 9. Differential (a)-(b) and common-mode (c) filter response. The electromagnetic (with and without losses) and circuit simulations of the filter responses have been inferred by means of the *Agilent ADS* commercial software, which includes the *Momentum* EM solver. The measurements have been obtained by means of the 4-port *Agilent PNA N5221A* network analyzer.
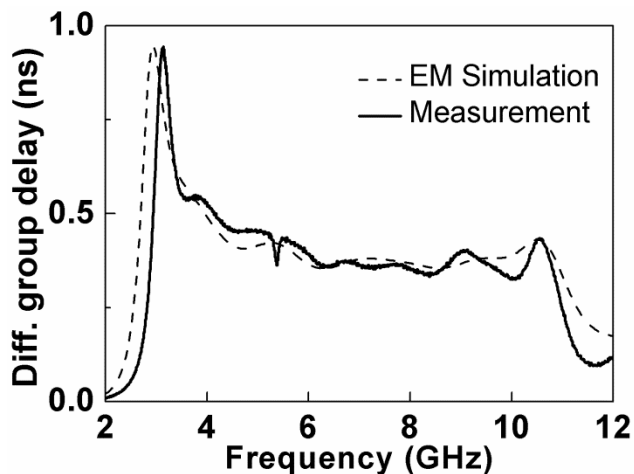
Fig. 10. Differential group delay of the filter of Fig.8.

V. COMPARISON TO OTHER APPROACHES

In order to appreciate the competitiveness, in terms of performance and dimensions, of the proposed balanced UWB bandpass filter with other similar filters reported in the literature, we summarize in table II some relevant parameters of such filters (we include some additional works, where balanced UWB responses with notched bands are included [20]-[22]). The filters reported in [13],[20],[21] exhibit strong common-mode rejection in the differential filter pass band, but size is large as compared to our filter. The other filters (including ours) exhibit comparable common-mode rejection, but the filter proposed in this work is much smaller. Exception is the filter proposed in [22], with strong common mode rejection in the differential filter pass band and small size. This filter is very competitive, although the reported band (with and without notched band) covers a smaller frequency range (between roughly 2 GHz and 7 GHz). By increasing the filter order, we would be able to accommodate more transmission zeros in the proposed balanced filters, and this can potentially improve the common-mode rejection level. Another possibility would be to load the central patch capacitances with additional SIRs oriented parallel to the filter axis (with the result of transmission zero splitting). This aspects will be investigated in future works.

TABLE II
COMPARISON OF VARIOUS DIFFERENTIAL UWB BANDPASS
FILTERS

Ref.	n	FBW(a) (%)	S_{21}^{CC} (dB) @ passband	Electrical Size	Dimension (mm)
[11]	6	117	>10	$0.93\lambda \times 2.12\lambda$	18.1 x 41.3
[12]	4	119	>9.6	$0.35\lambda \times 0.7\lambda$	10.4 x 20.4
[13]	-	123	>24	-	20 x 30
[14]	-	124	>13	$0.85\lambda \times 0.85\lambda$	28 x 28
[15]	-	135	>9	$1.9\lambda \times 2.4\lambda$	10.26 x 41
[20]	-	113	>13	0.57×0.57	-
[21]	-	139	>18.8	0.75×0.59	15.6 x 12.3
[22]	-	115	>22	0.56×0.28	24 x 12
This work	5	130	>10	$\mathbf{0.5\lambda \times 0.37\lambda}$	**10.5 x 7.6**

(a) FBW corresponding to the differential response.

Concerning the differential-mode response, the combination of in-band insertion and return loss and selectivity of the proposed filter is competitive, as compared to the other filters.

The filter reported in [11] exhibits comparable selectivity at the lower band edge and better selectivity at the upper band edge, but the measured in-band insertion loss is clearly better in the prototype reported in this work. In terms of in-band insertion losses, the filter reported in [15] is very competitive, but this filter is large and selectivity is limited. The filter reported in [12] exhibits a symmetric differential-mode response with very reasonable in-band insertion loss and significant selectivity at the upper transition band, but size is large, as compared to our prototype, and the selectivity at the lower transition band is much better in the filter designed in this work. Again, the filter proposed in [22] (without notched band) is very competitive concerning the differential mode in-band response and selectivity, but it is implemented in multilayer technology, and it does not cover the UWB regulated band from 3.1 GHz up to 10.6 GHz.

VI. CONCLUSIONS

In this paper, an ultra-compact microstrip order-5 balanced UWB bandpass filter with common-mode suppression has been designed and fabricated. The filter has been implemented by means of semi-lumped resonators, specifically, mirrored SIRs, patch capacitors and strip inductors, resulting in a device with compact size, as compared to other UWB balanced filters. To suppress the common-mode over the differential filter pass band, we have designed the three mirrored SIRs in order to provide different transmission zeros for that mode, distributed along the regulated UWB band. This has resulted in a filter with measured common-mode suppression higher than 10 dB. The measured differential-mode insertion and return losses of the fabricated prototype are better than 1.9 dB and 10 dB, respectively, within the whole UWB band. Hence, the combination of filter performance and size has been found to be competitive. An important aspect of this work is that a systematic design approach, based on the lumped element equivalent circuit models of the series and shunt branches, has been reported. Moreover, such circuit models, including parasitics, have been validated through full wave electromagnetic simulation, and it has been found that these circuits provide an accurate description of the structures up to very high frequencies (beyond the band of interest). The excellent agreement between the lossless electromagnetic simulation and circuit simulation of the designed filter for the differential-mode confirms and further supports the validity of the reported models.

REFERENCES

[1] C. H. Wu, C. H. Wang, and C. H. Chen, "Novel balanced coupled-line bandpass filters with common-mode noise suppression," *IEEE Trans. Microw. Theory Techn*., vol. 55, pp. 287-295, Feb. 2007.
[2] J. Shi, and Q. Xue, "Novel balanced dual-band bandpass filter using coupled stepped-impedance resonators," *IEEE Microw. Wireless Compon. Lett.*, vol. 20, pp. 19-21, Jan. 2010.
[3] J. Shi, and Q. Xue, "Dual-band and wide-stopband single-band balanced bandpass filters with high selectivity and common-mode suppression," *IEEE Trans. Microw. Theory Techn*., vol. 58, pp. 2204-2212, Aug. 2010.
[4] J. Shi, and Q. Xue, "Balanced bandpass filters using center-loaded half-wavelength resonators," *IEEE Trans. Microw. Theory Techn*., vol. 58, no. 4, pp. 970-977, Apr. 2010.

[5] C.-H. Lee, C.-I. G. Hsu, and C.-C. Hsu, "Balanced dual-band BPF with stub-loaded SIRs for common-mode suppression," *IEEE Microw. Wireless Compon. Lett.*, vol. 20, no. 2, pp. 70-73, Feb. 2010.

[6] C.-H. Wu, C.-H. Wang, and C. H. Chen, "Stopband-extended balanced bandpass filter using coupled stepped-impedance resonators," *IEEE Microw. Wireless Compon. Lett.*, vol 17, no. 7, pp. 507-509, Jul. 2007.

[7] C.-H. Wu, C.-H. Wang, and C. H. Chen, "Balanced coupled-resonator bandpass filters using multisection resonators for common-mode suppression and stopband extension," *IEEE Trans. Microw. Theory Techn.*, vol. 55, no. 8, pp. 1756–1763, Aug. 2007.

[8] A. Saitou, K. P. Ahn, H. Aoki, K. Honjo, and K. Watanabe, "Differential-mode bandpass filters with four coupled lines embedded in self complementary antennas," *IEICE Trans. Electron.*, vol. E90-C, no. 7, pp. 1524–1532, Jul. 2007.

[9] P. Vélez, J. Naqui, A. Fernández-Prieto, M. Durán-Sindreu, J. Bonache, J. Martel, F. Medina, and F. Martín, "Differential bandpass filter with common mode suppression based on open split ring resonators and open complementary split ring resonators," *IEEE Microwave and Wireless Components Letters*, vol. 23, no. 1, pp. 22-24, Jan. 2013.

[10] T. B. Lim, and L. Zhu, "A differential-mode wideband bandpass filter on microstrip line for UWB applications," *IEEE Microw. Wireless Compon. Lett.*, vol. 19, pp. 632-634, Oct. 2009.

[11] T. B. Lim and L. Zhu, "Differential-mode ultra-wideband bandpass filter on microstrip line," *Electron. Lett.*, vol.45, no.22, pp. 1124–1125, Oct. 2009.

[12] X-H. Wu, Q-X. Chu, "Compact differential ultra-wideband bandpass filter with common-mode suppression", *IEEE Microw. Wireless Compon. Lett.*, vol. 22, pp. 456-458, Sep. 2012.

[13] A. M. Abbosh, "Ultrawideband balanced bandpass filter", *IEEE Microw. Wireless Compon. Lett.*, vol. 21, pp. 480-482, Sep. 2011.

[14] H. T. Zhu, W. J. Feng, W. Q. Che and Q. Xue, "Ultra-wideband differential bandpass filter based on transversal signal-interference concept", *Electronic Letters*, vol.47,Sep. 2011

[15] X.-H. Wang, H. Zhang and B.-Z. Wang, "A novel ultra-wideband differential filter based on microstrip line structures", *IEEE Microw. Wireless Compon. Lett.*, vol. 23, pp. 128-130, March. 2013.

[16] P. Vélez, J. Naqui, M. Durán-Sindreu, J.Bonache, A. Fernández Prieto, J. Martel, F. Medina and F. Martín, "Differential bandpass Filters with Common-Mode Suppression based on Stepped Impedance Resonators (SIRs)", *IEEE MTT-S Int. Microwave Symp.*, June 2013, Seattle (USA).

[17] D. M. Pozar, *Microwave Engineering*, AddisonWesley, 1980.

[18] J. S. Hong and M. J. Lancaster, *Microstrip Filters for RF/Microwave Applications*, John Wiley & Sonc Inc., 2001.

[19] R. A. Foster, "A reactance theorem," Bell Syst. Tech. J., vol. 3, pp. 259–267, Apr. 1924.

[20] S. Shi, W.-W. Choi, W. Che, K.-W- Tam and Q. Xue, "Ultra-wide-band differential bandpass filter with narrow notched band and improved common-mode suppression by DGS," *IEEE Microw. Wireless Compon. Lett.*, vol. 22, no. 4, pp. 185-187, Apr. 2012.

[21] C-H Lee, C-I.G. Hsu, and C-J. Chen, "Band-notched balanced uwb bpf with stepped-impedance slotline multi-mode resonator," *IEEE Microw. Wireless Compon. Lett.*, vol. 22, no.4, pp. 182-184, Apr. 2012.

[22] J. Shi, C. Shao, J-X. Chen, Q-Y. Lu, Y. Peng, and Z-H. Bao, "Compact low-loss wideband differential bandpass filter with high common-mode suppression", *IEEE Microw. Wireless Compon. Lett.*, vol. 23, no. 9, pp. 480-482, Sep. 2013.

Jordi Naqui (S'11-M'14) was born in Granollers, Spain. He received by the Universitat Autònoma de Barcelona (UAB) the Telecommunication Technical Engineering diploma (specialty in Electronics) in 2006, the Telecommunication Engineering degree in 2010, the Master's degree in Micro and Nanoelectronics Engineering in 2011, and the PhD degree in Electronics Engineering in 2014. He was awarded with a predoctoral teaching and research fellowship by the Spanish Government from 2011 to 2014. Currently, he is a postdoctoral researcher and teacher of the research center CIMITEC at the UAB. His research activities are mainly focused on circuit modeling and design of passive microwave resonant structures, including filters, sensors, and chipless RFID tags.

Armando Fernández Prieto (S'11) was born in Ceuta, Spain, in September 1981. He recieved the Licenciado and Ph.D. degrees from the University of Seville, Spain, in 2007 and 2013, respectively, both in physics. His research interests focus on printed passive microwave filters, couplers and metamaterials. Dr. Fernández is a reviewer of the IEEE TRANSACTIONS ON MICROWAVE THEORY AND TECHNIQUES and of many other journals.

Jordi Bonache (S'05–M'07) was born in 1976 in Barcelona, Spain. He received the Physics and Electronics Engineering degrees and the Ph.D. degree in electronics engineering from the Universitat Autònoma de Barcelona, Barcelona, Spain, in 1999, 2001, and 2007, respectively. In 2000, he joined the "High Energy Physics Institute" of Barcelona (IFAE), where he was involved in the design and implementation of the control and monitoring system of the MAGIC telescope. In 2001, he joined the Department of Electronics Engineering of the Universitat Autònoma de Barcelona where he is currently Lecturer. From 2006 to 2009 he worked as executive manager of CIMITEC. Currently he is leading the research in RFID and antennas in CIMITEC. His research interests include active and passive microwave devices, metamaterials, antennas and RFID.

Javier Mata Contreras was born in 1976 in Málaga (Spain). He received the Ingeniería de Telecomunicación Degree from the Universidad de Málaga (UMA) in 2000 and the PhD degree from the same university in 2010, with the Thesis "Distributed Amplifiers and Mixers with Transmission Lines based on Metamaterials" . In 2000, he joined the UMA Department of Ingeniería de Comunicaciones as Assistant Professor. He is currently working at CIMITEC and the Universitat Autònoma de Barcelona (UAB) as Visitant Professor. His research interests include active and passive microwave devices and active distributed circuits based on metamaterials, among others.

Jesús Martel (M'08) received the Licenciado and Doctor degrees in Physics from the University of Seville, in 1989 and 1996, respectively. Since 1990 he has developed his research work in the Microwave Group of the University of Seville. In 1992, he joined the Department of Applied Physics II, University of Seville, where, in 2000, he became an Associate Professor and, in 2010, Head of the Department. His current research interest is focused on the numerical analysis of planar transmission lines, the modeling of planar microstrip discontinuities, the design of passive microwave circuits, microwave measurements, and artificial media.

Francisco Medina (M'90–SM'01–F'10) was born in Puerto Real, Cádiz, Spain, in November 1960. He received the Licenciado and Ph.D. degrees from the University of Sevilla, Seville, Spain, in 1983 and 1987, respectively, both in Physics. He is currently a Professor of Electromagnetism with the Department of Electronics and Electromagnetism, University of Sevilla, Seville, Spain, and Head of the Microwaves Group. His research

Paris Vélez (S'10-M'14) was born in Barcelona (Spain) in 1982. He received the degree in Telecommunications Engineering, specializing in Electronics in 2008 and the Electronics Engineering degree in 2010 from the Universitat Autònoma de Barcelona. In 2014 he received his PhD in Electrical Engineering from the UAB with a thesis entitled "Common mode suppression differential microwave circuits based on Metamaterial concepts and semilumped resonators". During the PhD he was awarded with a predoctoral teaching and research fellowship by the Spanish Government from 2011 to 2014. Dr. Vélez is a reviewer of the IEEE T-MTT and of other journals. Actually, his scientific activity is focused on the miniaturization of passive circuits RF / microwave based Metamaterials.

interest includes analytical and numerical methods for planar structures, anisotropic materials, and artificial media modeling. He has coauthored more than 130 book chapters and journal papers on those topics as well as more than 260 conference contributions. He acts as reviewer for more than 40 IEEE, IEE, AIP and IoP journals and he has been member of the TPCs of a number of local and international conferences. He is now Associate Editor of the International Journal of Microwave and Wireless Technologies.

Ferran Martín (M'04-SM'08-F'12) was born in Barakaldo (Vizcaya), Spain in 1965. He received the B.S. Degree in Physics from the Universitat Autònoma de Barcelona (UAB) in 1988 and the PhD degree in 1992. From 1994 up to 2006 he was Associate Professor in Electronics at the Departament d'Enginyeria Electrònica (Universitat Autònoma de Barcelona), and since 2007 he is Full Professor of Electronics. In recent years, he has been involved in different research activities including modelling and simulation of electron devices for high frequency applications, millimeter wave and THz generation systems, and the application of electromagnetic bandgaps to microwave and millimeter wave circuits. He is now very active in the field of metamaterials and their application to the miniaturization and optimization of microwave circuits and antennas. He is the head of the Microwave Engineering, Metamaterials and Antennas Group (GEMMA Group) at UAB, and director of CIMITEC, a research Center on Metamaterials supported by TECNIO (Generalitat de Catalunya). He has organized several international events related to metamaterials, including Workshops at the IEEE International Microwave Symposium (years 2005 and 2007) and European Microwave Conference (2009), and the Fifth International Congress on Advanced Electromagnetic Materials in Microwaves and Optics (Metamaterials 2011), where he has acted as chair of the Local Organizing Committee. He has acted as Guest Editor for three Special Issues on Metamaterials in three International Journals. He has authored and co-authored over 450 technical conference, letter, journal papers and book chapters, he is co-author of the book on Metamaterials entitled Metamaterials with Negative Parameters: Theory, Design and Microwave Applications (John Wiley & Sons Inc.), and he has generated 14 PhDs. Ferran Martín has filed several patents on metamaterials and has headed several Development Contracts.
Prof. Martín is a member of the IEEE Microwave Theory and Techniques Society (IEEE MTT-S). He is reviewer of the IEEE Transactions on Microwave Theory and Techniques and IEEE Microwave and Wireless Components Letters, among many other journals, and he serves as member of the Editorial Board of IET Microwaves, Antennas and Propagation and International Journal of RF and Microwave Computer-Aided Engineering. He is also a member of the Technical Committees of the European Microwave Conference (EuMC) and International Congress on Advanced Electromagnetic Materials in Microwaves and Optics (Metamaterials). Among his distinctions, Ferran Martín has received the 2006 Duran Farell Prize for Technological Research, he holds the Parc de Recerca UAB – Santander Technology Transfer Chair, and he has been the recipient of two ICREA ACADEMIA Awards (calls 2008 and 2013).